

## Antenna and pulse selection for colocated MIMO radar

Tohidi, Ehsan; Behroozi, Hamid; Leus, Geert

**DOI**

[10.1109/ACSSC.2017.8335404](https://doi.org/10.1109/ACSSC.2017.8335404)

**Publication date**

2018

**Document Version**

Final published version

**Published in**

Conference Record of the 51st Asilomar Conference on Signals, Systems and Computers, ACSSC 2017

**Citation (APA)**

Tohidi, E., Behroozi, H., & Leus, G. (2018). Antenna and pulse selection for colocated MIMO radar. In M. B. Matthews (Ed.), *Conference Record of the 51st Asilomar Conference on Signals, Systems and Computers, ACSSC 2017* (pp. 563-567). IEEE. <https://doi.org/10.1109/ACSSC.2017.8335404>

**Important note**

To cite this publication, please use the final published version (if applicable).  
Please check the document version above.

**Copyright**

Other than for strictly personal use, it is not permitted to download, forward or distribute the text or part of it, without the consent of the author(s) and/or copyright holder(s), unless the work is under an open content license such as Creative Commons.

**Takedown policy**

Please contact us and provide details if you believe this document breaches copyrights.  
We will remove access to the work immediately and investigate your claim.

***Green Open Access added to TU Delft Institutional Repository***

***'You share, we take care!' - Taverne project***

**<https://www.openaccess.nl/en/you-share-we-take-care>**

Otherwise as indicated in the copyright section: the publisher is the copyright holder of this work and the author uses the Dutch legislation to make this work public.

# Antenna and Pulse Selection for Colocated MIMO Radar

Ehsan Tohidi\*, Hamid Behroozi\*, and Geert Leus†

\*Sharif University of Technology, Tehran, Iran.

†Delft University of Technology, Delft, The Netherlands.

E-mails: tohidi@ee.sharif.edu, behroozi@sharif.edu, g.j.t.leus@tudelft.nl.

**Abstract**—Multiple input multiple output (MIMO) radar is known for its superiority over conventional radar due to its antenna and waveform diversity. However, the increased hardware cost (due to multiple transmitters and receivers), power consumption (due to multiple transmitters and pulses), and computational complexity (due to numerous pulses) form the drawbacks of MIMO radar. On one hand, a higher estimation accuracy is required, but on the other hand, a lower number of active antennas/pulses is desirable. Therefore, in this paper, by proposing a convex optimization approach for the general case of transmitter-receiver-pulse selection, we will minimize the total number of active antennas/pulses in order to guarantee a prescribed performance accuracy. The performance measure we will optimize is the Cramér-Rao lower bound (CRLB) for the angle and velocity estimation accuracy of two targets, which provides a trade-off between the main beamwidth and the sidelobe level (SLL) of the ambiguity function.

## I. INTRODUCTION

Colocated multiple input multiple output (MIMO) radar is a MIMO radar with closely spaced antennas which implies that different transmitter-receiver pairs see a target from nearly the same angular view. Multiple antennas besides waveform diversity result in higher angular resolution, parameter identifiability, and target detection in colocated MIMO radar. In [1], the Cramér-Rao lower bound (CRLB) for a MIMO radar is derived to prove the improved estimation of the targets' angle of arrival and velocity. On the other hand, hardware cost (due to multiple antennas), energy consumption (due to multiple transmitted pulses by multiple transmitters), and computational complexity (due to the huge number of samples related to multiple transmitters, pulses, and receivers) are the main disadvantages of these radars. Applying compressive sensing (CS) to radar aiming at reducing the number of measurements and thus the computational complexity has been vastly studied [2, 3]. Although CS reduces the number of measurements, the number of samples (i.e., antennas and pulses) remains unchanged. Sparse sensing is an approach to directly reduce the number of samples. The samples are selected sparsely in such a way that the required tasks could still be done properly.

Sparse sensing in the spatial domain is called sensor selection (or antenna selection) where a subset of the set of candidate sensors is selected. A convex optimization based sensor selection algorithm is proposed in [4], where the problem is relaxed to a convex program first, and then, sensors are selected through a convex optimization. In [5], sensor selection for general non-linear models through convex optimization is presented. Similar to sensor selection, antenna and pulse

selection is the problem of choosing a subset of reference antennas and pulses. Antenna placement in widely separated MIMO radar for joint target position and velocity estimation is studied in [6–8], which are all based on the single-target CRLB.

The aim of this paper is to select the optimal set of antennas and pulses that guarantees a desired estimation accuracy for the angle of arrival (AOA) and velocity. A reduction in the number of antennas and pulses results in a reduction in hardware complexity, energy consumption, and computational complexity. In addition, we introduce a two-target CRLB as a better performance measure for parameter estimation since it considers both the mainlobe width and sidelobe level of the ambiguity function.

The rest of the paper is organized as follows. The problem statement is given in Section II. Two illustrative examples are explained in Section III. In Section IV, the proposed algorithm is presented. Section V is dedicated to the numerical results. Finally, Section VI concludes the paper.

## II. PROBLEM STATEMENT

We consider a colocated MIMO radar with  $I$  transmitters and  $R$  receivers along a line at coordinates  $[-d, -2d, \dots, -Id]$  and  $[d, 2d, \dots, Rd]$ , respectively, where  $d$  is inter-element spacing, which is assumed to be  $\lambda/2$  where  $\lambda$  is the signal wavelength. The waveform of the  $i$ th transmitter is  $s_i(t)$  which is transmitted  $P$  times with a pulse repetition interval (PRI),  $T_P$ . The baseband representation of the  $p$ th pulse received at the  $r$ th receiver during the time interval  $[pT_P, (p+1)T_P]$  is given by

$$x_r(t) = \sum_{q=1}^Q \sum_{i=1}^I \alpha_q s_i(t - pT_P - \tau_{i,r}^q) \exp(-j2\pi f_c \tau_{i,r}^q) \exp(j2\pi f_d^q t) + e_r(t), \quad (1)$$

where  $Q$  is the number of targets in the region of interest,  $\alpha_q$  is the radar cross section (RCS) of the  $q$ th target, and  $f_c$  is the carrier frequency, i.e.,  $f_c = c/\lambda$  with  $c$  the light speed. Next,  $\tau_{i,r}^q = c^{-1}[2R_q - (d_i + d_r)u_q]$  is the propagation delay of the signal transmitted from the  $i$ th transmitter, reflected by the  $q$ th target and received at the  $r$ th receiver, where  $R_q$  is the  $q$ th target distance from the array center,  $d_i$  and  $d_r$  are the position of the  $i$ th transmitter and the  $r$ th receiver, respectively, and  $u_q = \cos\theta_q$  is the direction cosine of the  $q$ th target AOA. Further,  $f_d^q = \frac{2v_q}{\lambda}$  is the Doppler frequency of the  $q$ th target with  $v_q$  being its velocity. Finally,  $e_r(t)$  is the received noise

at the  $r$ th receiver. We assume that all transmit signals are orthogonal to each other [9].

Henceforth, employing  $I$  matched filters matched to the  $I$  transmit waveforms, the observed signal due to the  $(i, r)$  transmitter-receiver pair is given by

$$z_{r,i}(t) = \sum_{q=1}^Q \alpha_q \exp(j2\pi \frac{(d_i + d_r)u_q}{\lambda}) \exp(j4\pi \frac{v_q}{\lambda} t) + e_{r,i}(t), \quad (2)$$

where  $e_{r,i}(t)$  is the noise term at the output of the  $i$ th matched filter at the  $r$ th receiver. Since all  $I$  transmit waveforms are orthogonal, the noise terms can be assumed to be independent. Thus,  $e_{r,i}(t), r = 1, \dots, R, i = 1, \dots, I$ , are modeled as i.i.d. with distribution  $\mathcal{N}(0, \sigma_e^2)$ . Sampling the observed signal with sampling interval  $T_s$ ,  $N$  samples per pulse are obtained, where the  $n$ th sample of the  $p$ th pulse related to the transmitter-receiver pair  $(i, r)$  is given by

$$\begin{aligned} z_{r,i,p}[n] &= z_{r,i,p}(pT_P + nT_s) \\ &= \sum_{q=1}^Q \alpha_q \exp(j2\pi \frac{d_i + d_r}{\lambda} u_q) \exp(j4\pi \frac{nT_s + pT_P}{\lambda} v_q) \\ &\quad + e_{r,i,p}(nT_s + pT_P) = y_{r,i,p}[n] + e_{r,i,p}[n]. \end{aligned} \quad (3)$$

Collecting all the measurements, we have a non-linear model of the form

$$\mathbf{z} = \mathbf{y}(\boldsymbol{\theta}) + \mathbf{e} \in \mathbb{C}^{NRIP}, \quad (4)$$

where  $\boldsymbol{\theta} = [\boldsymbol{\theta}_1^T, \dots, \boldsymbol{\theta}_Q^T]^T \in \mathbb{R}^{2Q}$  is the vector of all unknown parameters with  $\boldsymbol{\theta}_q = [u_q, v_q]^T \in \mathbb{R}^2$  collecting the unknown parameters of the  $q$ th target.

#### A. Performance measures

Since the CRLB is a lower bound for all unbiased estimators and always can be expressed in closed form, we employ the CRLB as a benchmark for the selection problem. The covariance of any unbiased estimate  $\hat{\boldsymbol{\theta}}$  of the unknown parameter satisfies the following inequality [5, 10]

$$\mathbb{E}\{(\boldsymbol{\theta} - \hat{\boldsymbol{\theta}})(\boldsymbol{\theta} - \hat{\boldsymbol{\theta}})^H\} \geq \mathbf{C}(\boldsymbol{\theta}) = \mathbf{F}^{-1}(\boldsymbol{\theta}), \quad (5)$$

where  $\mathbf{C}$  is the CRLB matrix and  $\mathbf{F}$  is the Fisher information matrix (FIM), which can be calculated as [5]

$$\mathbf{F}(\boldsymbol{\theta}) = \mathbb{E} \left\{ \frac{\partial \ln p(\mathbf{z}; \boldsymbol{\theta})}{\partial \boldsymbol{\theta}} \frac{\partial \ln p(\mathbf{z}; \boldsymbol{\theta})}{\partial \boldsymbol{\theta}^H} \right\} \in \mathbb{C}^{2Q \times 2Q}, \quad (6)$$

where  $p(\mathbf{z}; \boldsymbol{\theta})$  is the probability density function (pdf) of  $\mathbf{z}$  parameterized by the unknown vector  $\boldsymbol{\theta}$ . Since uncorrelated errors are assumed, the log-likelihood  $\ln p(\mathbf{z}; \boldsymbol{\theta})$  is additive. The log-likelihood for (4) is hence given by

$$\ln p(\mathbf{z}; \boldsymbol{\theta}) = \sum_{r=1}^R \sum_{i=1}^I \sum_{p=1}^P \sum_{n=1}^N \ln p(z_{r,i,p}[n]; \boldsymbol{\theta}). \quad (7)$$

Therefore, (6) can be rewritten in the following form [5]

$$\mathbf{F}(\boldsymbol{\theta}) = \sum_{r=1}^R \sum_{i=1}^I \sum_{p=1}^P \mathbf{F}_{r,i,p}(\boldsymbol{\theta}), \quad (8)$$

where  $\mathbf{F}_{r,i,p}(\boldsymbol{\theta})$  is the FIM of the  $p$ th pulse due to the transmitter-receiver pair  $(i, r)$  for all the  $N$  samples, i.e.,

$$\mathbf{F}_{r,i,p}(\boldsymbol{\theta}) = \sum_{n=1}^N \mathbf{F}_{r,i,p,n}(\boldsymbol{\theta}) = \frac{4}{\sigma_e^2} \sum_{n=1}^N \frac{\partial y_{r,i,p}[n]}{\partial \boldsymbol{\theta}} \frac{\partial y_{r,i,p}[n]}{\partial \boldsymbol{\theta}^H}. \quad (9)$$

The CRLB derived for one target is usually employed as the estimation accuracy criterion. In this paper, we choose the two-target CRLB as a better measure in comparison with the single-target CRLB. As will be shown later, in contrast to the single-target CRLB which only considers estimation accuracy, the two-target CRLB also includes the ambiguity due to the existence of two targets. For the sake of brevity, we do not present the CRLB derivation here. It can be shown that the expression for the single-target CRLB is independent of  $\boldsymbol{\theta}$ . Although unknown parameters appear in the two-target CRLB, the expression only depends on the difference of parameters, i.e.,  $v_1 - v_2$  and  $u_1 - u_2$  or more generally  $\delta\boldsymbol{\theta} = \delta\boldsymbol{\theta}_1 - \delta\boldsymbol{\theta}_2$ .

As the CRLB is a matrix, we cannot use it directly as an objective function of an optimization problem. We employ the following functions as scalar measures of the estimation accuracy:

- A-optimality: minimize the sum of eigenvalues, i.e.,  $f(\mathbf{C}) = \text{tr}\{\mathbf{C}\}$ .
- E-optimality: minimize the maximum eigenvalue, i.e.,  $f(\mathbf{C}) = \lambda_{\max}\{\mathbf{C}\}$ .

Since the single-target CRLB is independent of the unknown parameters, we only need to calculate it once. On the other hand, for the two-target CRLB, we need to consider all parameter differences in a region of interest. Thus, we discretize the unknown parameter difference region of interest into a set of grid points,  $\mathcal{D} = \{\delta\boldsymbol{\theta}_1, \dots, \delta\boldsymbol{\theta}_D\}$  and we consider these points in our optimization problem.

#### B. Problem formulation

We model the sensing framework by introducing the transmitter-pulse selection matrix  $\mathbf{A} \in \{0, 1\}^{I \times P}$ , where the  $(i, p)$ th entry of  $\mathbf{A}$  denoted by  $A_{i,p}$  is equal to 1(0) if the  $i$ th transmitter transmits the  $p$ th pulse (or not). The receiver selection vector  $\mathbf{b} \in \{0, 1\}^R$  is defined in a similar way. Considering these selection parameters, the measurements in (3) can be rewritten as follows

$$z_{r,i,p}[n] = b_r \times A_{i,p} \times (y_{r,i,p}[n] + e_{r,i,p}[n]), \quad (10)$$

where depending on whether a transmitter-receiver-pulse is selected, the measurement will be collected. It is easy to show that the FIM will be modified based on (10) as

$$\mathbf{F}(\mathbf{A}, \mathbf{b}, \delta\boldsymbol{\theta}) = \sum_{r=1}^R b_r \sum_{i=1}^I \sum_{p=1}^P A_{i,p} \mathbf{F}_{r,i,p}(\delta\boldsymbol{\theta}). \quad (11)$$

The most general form of the optimization problem can be mathematically formulated as

$$\begin{aligned} \max_{\mathbf{A}, \mathbf{b}} \quad & \min_{\delta\boldsymbol{\theta} \in \mathcal{D}} f(\mathbf{A}, \mathbf{b}, \delta\boldsymbol{\theta}) \\ \text{subject to} \quad & \mathbf{A} \in \mathcal{A}, \mathcal{A} = \{\mathbf{A} | A_{i,p} \in \{0, 1\}, i = 1, \dots, I, \\ & p = 1, \dots, P, \|\mathbf{A}\|_0 = K_P\}, \\ & \mathbf{b} \in \mathcal{B}, \mathcal{B} = \{\mathbf{b} | b_r \in \{0, 1\}, r = 1, \dots, R, \\ & \|\mathbf{b}\|_0 = K_R\}, \end{aligned} \quad (12)$$

where  $f(\mathbf{A}, \mathbf{b}, \delta\boldsymbol{\theta})$  is a function of the FIM  $\mathbf{F}(\mathbf{A}, \mathbf{b}, \delta\boldsymbol{\theta})$  at grid points  $\delta\boldsymbol{\theta} \in \mathcal{D}$  and the sets  $\mathcal{A}$  and  $\mathcal{B}$  represent the sensing constraints.

### III. ILLUSTRATIVE EXAMPLES

In this section, we present the concept of pulse and antenna selection by showing two illustrative examples. In addition, the superiority of the two-target CRLB over the single-target CRLB is shown. Here, small-scale examples are presented and the selection is done by an exhaustive search. A-optimality is selected as performance measure, i.e.,  $f(\mathbf{A}, \mathbf{b}, \delta\boldsymbol{\theta}) = \text{tr}\{\mathbf{F}^{-1}(\mathbf{A}, \mathbf{b}, \delta\boldsymbol{\theta})\}$ . We study two special cases: pulse selection for a radar with a single transmitter-receiver pair and antenna selection for a MIMO radar with a single pulse. The convex optimization based algorithm is presented in Section IV.

First, we consider the example of pulse selection for a radar with a single transmitter-receiver pair, which is able to transmit  $P$  identical pulses. We are aiming at comparing the estimation accuracy for different numbers of selected pulses. Since there is no angle estimation, we only consider velocity as the unknown parameter. The selection is done through an exhaustive search on all the possible combinations of pulses considering both the single and two-target CRLB. In the following figures, the effect of pulse selection on the estimation error is presented, where we consider 12 pulses in total. The result for the selection of 5 and 8 pulses for both the single- and two-target CRLB is depicted in Figure 1(a). As expected, the selected pulses for the single-target CRLB criterion are towards the edges. However, for the two-target CRLB case, pulses from both the edges and the middle of the pulse sequence are selected. This difference in pulse selection policy results in different velocity ambiguity function plots, see Figure 1(b). As shown, the sidelobe level of the ambiguity function for the two-target CRLB is lower especially for the ones close to the main lobe. Of course, this sidelobe reduction is achieved at the price of a wider beamwidth in comparison with the single-target CRLB ambiguity function.

For the second example, we study the effect of antenna selection on the target angle estimation accuracy. Here we consider multiple transmitters and multiple receivers with a single transmit pulse,  $P = 1$ . Therefore, the target direction cosine is the unknown parameter and the target velocity is ignored for this scenario. An exhaustive search is performed to determine the optimum selection of transmitters and receivers. A scenario with a total of 8 transmitters and 4 receivers is considered. The results of the selection of 4 transmitters combined with 3 receivers and 6 transmitters combined with 2 receivers for both the single- and two-target CRLB are depicted in Figure 2. The selected antennas are depicted in

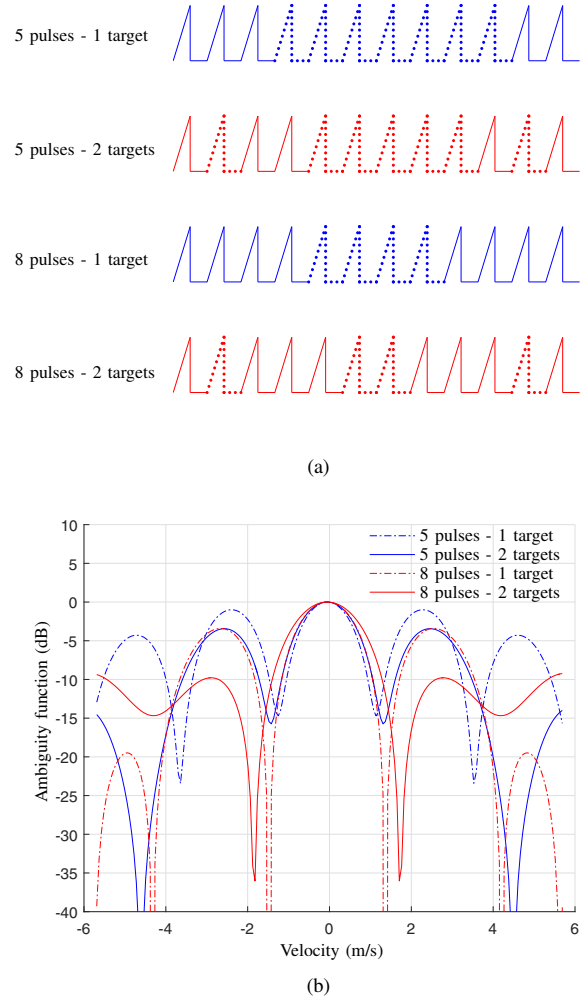


**Fig. 1:** Single antenna pulse selection based on velocity estimation error for a total of  $P = 12$  pulses (a) selected pulses, (b) velocity ambiguity function.

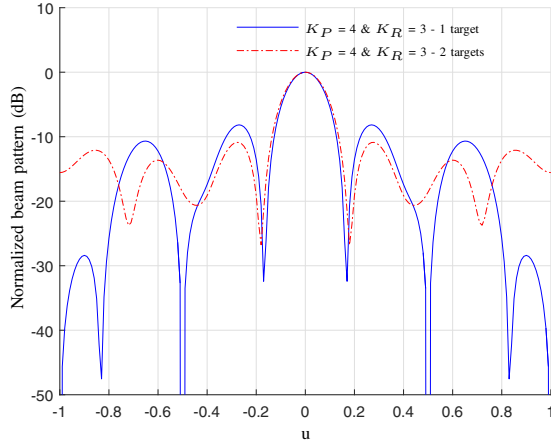
Figure 2(a). The selected antennas based on the single-target CRLB appear towards the edges, however in the two-target CRLB case, antennas are selected from both the edges and middle of the antenna array. This result is well aligned with the pulse selection for the single antenna example. Figures 2(b) and 2(c) compare the beampatterns of the single- and two-target CRLB. As shown, the ambiguity function beamwidth is traded off with the sidelobe level (especially, for the sidelobes close to the mainlobe) in the two-target CRLB in comparison with the single-target CRLB.

### IV. PROPOSED METHOD

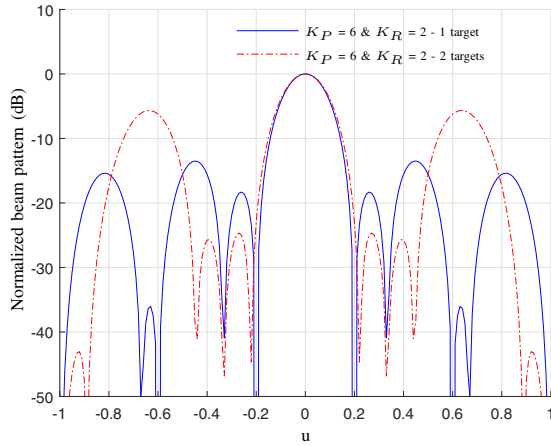
In this section, we study the general case of transmitter-receiver-pulse selection. We propose a convex optimization approach for the selection problem. We consider E-optimality as the scalar measure, i.e.,  $f(\mathbf{A}, \mathbf{b}, \delta\boldsymbol{\theta}) = \lambda_{\max}\{\mathbf{F}^{-1}(\mathbf{A}, \mathbf{b}, \delta\boldsymbol{\theta})\}$ . By relaxing the Boolean constraints in (12), the optimization



(a)



(b)



(c)

**Fig. 2:** MIMO radar antenna selection based on angle estimation error for a total of 8 transmitters and 4 receivers (a) Selected antennas, (b) beampatterns for 4 transmitters and 3 receivers, (c) beampatterns for 6 transmitters and 2 receivers.

problem could be written in the epigraph form as

$$\begin{aligned}
 & \max_{\mathbf{A}, \mathbf{b}, \gamma} \gamma \\
 & \text{subject to } \mathbf{F}(\mathbf{A}, \mathbf{b}, \delta\boldsymbol{\theta}) \geq \gamma \mathbf{I}_{4 \times 4}, \forall \delta\boldsymbol{\theta} \in \mathcal{D} \\
 & \sum_{i=1}^I \sum_{p=1}^P A_{ip} \leq K_P, \\
 & \sum_{r=1}^R b_r \leq K_R, \\
 & 0 \leq A_{ip} \leq 1, 1 \leq i \leq I, 1 \leq p \leq P, \\
 & 0 \leq b_r \leq 1, 1 \leq r \leq R.
 \end{aligned} \tag{13}$$

where  $\mathbf{F}(\mathbf{A}, \mathbf{b}, \delta\boldsymbol{\theta})$  is the FIM,  $\mathbf{A}$  and  $\mathbf{b}$  are the selection matrix and selection vector defined in (11), respectively, and  $K_P$  and  $K_R$  are the number of selected pulses and receivers, respectively. Multiplication of the unknown parameters ( $\mathbf{A}$  and  $\mathbf{b}$ ) in  $\mathbf{F}$ , implies the non-convexity of (13). Thus, we present a convexifying process by introducing new optimization parameters. First, we define a pulse selection vector by vectorizing the selection matrix (i.e.,  $\mathbf{a} = \text{vec}(\mathbf{A})$ ). Then, we introduce the total selection vector  $\mathbf{w}$  by concatenating both the pulse and receiver selection vectors,  $\mathbf{w} = [\mathbf{a}^T, \mathbf{b}^T]^T$ . Finally, the total selection matrix is defined as  $\mathbf{W} = \mathbf{w}\mathbf{w}^T$  which eliminates the multiplication of the unknowns. In addition, by applying some standard convex relaxations, we relax the only non-convex term  $\mathbf{W} = \mathbf{w}\mathbf{w}^T$ . The relaxed convex optimization problem can be stated as

$$\begin{aligned}
 & \max_{\mathbf{W}, \mathbf{w}, \gamma} \gamma \\
 & \text{subject to } \mathbf{F}(\mathbf{W}, \delta\boldsymbol{\theta}) \geq \gamma \mathbf{I}_{4 \times 4}, \forall \delta\boldsymbol{\theta} \in \mathcal{D}, \\
 & \begin{bmatrix} \mathbf{W} & \mathbf{w} \\ \mathbf{w}^T & 1 \end{bmatrix} \succeq \mathbf{0}, \\
 & W_{i,j} = W_{j,i}, 1 \leq i, j \leq IP + R, \\
 & W_{i,i} = w_i, 1 \leq i \leq IP + R, \\
 & \sum_{i=1}^{IP} w_i \leq K_P, \\
 & \sum_{r=IP+1}^{IP+R} w_r \leq K_R, \\
 & 0 \leq w_i \leq 1, 1 \leq i \leq I \times P + R.
 \end{aligned} \tag{14}$$

The optimization problem in (14) is a standard semidefinite programming problem in the inequality form which can be efficiently solved in polynomial time using interior-point methods. In this paper, we employed CVX to solve (14). To compute the suboptimal Boolean solution from the relaxed optimization problem, we employ randomized rounding which selects the antennas and pulses with a probability equal to the output of the convex problem [5].

## V. SIMULATION RESULTS

In this section, the performance of the proposed algorithm is evaluated through numerical simulations. In total, we consider 4 receivers, 4 transmitters, and 4 pulses. Figure 3 presents the MSE of the optimization algorithm in comparison with the optimum MSE plot. The results are plotted for two different cases. In the first case, one out of four receivers is selected and in the second case, three out of four receivers

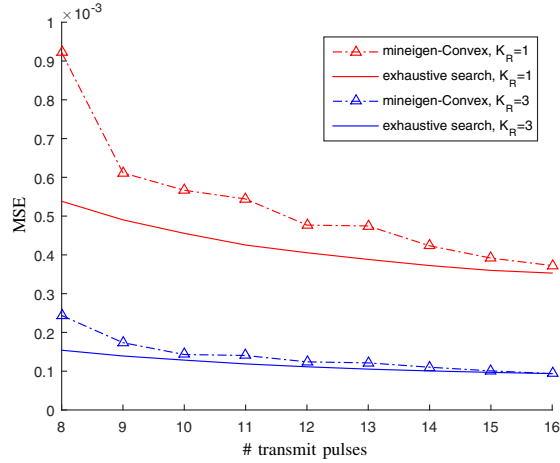


**Fig. 3:** MSE versus number of transmit pulses for different approaches.

are selected. It is shown that the achieved MSE is not much far from the optimum value. As expected, by increasing the number of receivers or transmit pulses, the MSE decreases. However, it reduces slightly after some point. Moreover, Figure 4 presents the result of the proposed algorithm when 12 pulses and 3 receivers are selected. The resulting ambiguity function and selected transmitters, receivers, and pulses are depicted in Figures 4(a) and 4(b), respectively.

## VI. CONCLUSIONS

In this paper, we studied antenna and pulse selection for a colocated MIMO radar with multiple transmit pulses aiming at a reduction in hardware cost and energy consumption. Scalar measures of the CRLB were employed as the objective function. It was shown that the two-target CRLB is a better metric in comparison with the single-target CRLB since it considers both the estimation accuracy and ambiguity due to two targets. Moreover, a convex optimization approach was proposed to obtain a proper selection mechanism. Finally, it was verified through simulations that, although the MSE increases by decreasing the number of antennas and pulses, it is possible to decrease the number of antennas and pulses with only a slight reduction in performance.

## REFERENCES

- [1] Q. He, J. Hu, R. S. Blum, and Y. Wu, "Generalized Cramér-Rao Bound for Joint Estimation of Target Position and Velocity for Active and Passive Radar Networks," *IEEE Trans. Signal Process.*, vol. 64, pp. 2078–2089, April 2016.
- [2] J. Ender, "A brief review of compressive sensing applied to radar," in *Proc. 14th International Radar Symposium (IRS)*, vol. 1, pp. 3–16, June 2013.
- [3] E. Tohidi, M. Radmard, S. M. Karbasi, H. Behroozi, and M. M. Nayebi, "Compressive sensing in MTI processing," in *Proc. 3rd International Workshop on Compressed Sensing Theory and its Applications to Radar, Sonar and Remote Sensing (CoSeRa)*, pp. 189–193, June 2015.
- [4] S. Joshi and S. Boyd, "Sensor selection via convex optimization," *IEEE Trans. Signal Process.*, vol. 57, pp. 451–462, Feb 2009.

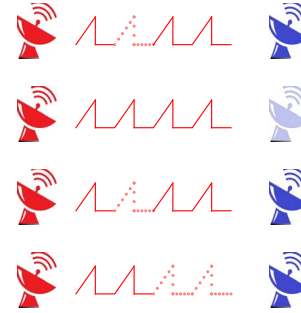
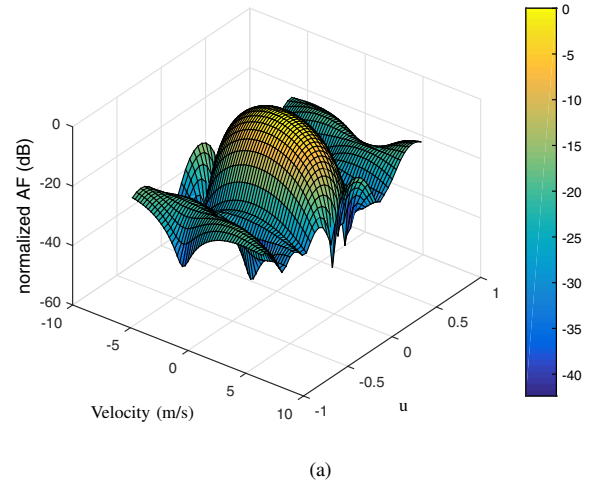


**Fig. 4:** Convex optimization for 12 pulses and 3 receivers (a) angle-velocity ambiguity function, (b) selected transmitters-pulses-receivers.

- [5] S. P. Chepuri and G. Leus, "Sparsity-promoting sensor selection for non-linear measurement models," *IEEE Trans. Signal Process.*, vol. 63, pp. 684–698, Feb 2015.
- [6] Q. He, R. S. Blum, H. Godrich, and A. M. Haimovich, "Target velocity estimation and antenna placement for mimo radar with widely separated antennas," *IEEE J. Sel. Topics Signal Process.*, vol. 4, pp. 79–100, Feb 2010.
- [7] M. S. Greco, P. Stinco, F. Gini, and A. Farina, "Cramér-Rao bounds and selection of bistatic channels for multistatic radar systems," *IEEE Trans. Aerosp. Electron. Syst.*, vol. 47, pp. 2934–2948, OCTOBER 2011.
- [8] I. Ivashko, G. Leus, and A. Yarovoy, "Radar network topology optimization for joint target position and velocity estimation," *Signal Processing*, vol. 130, pp. 279–288, 2017.
- [9] Q. He, R. S. Blum, and A. M. Haimovich, "Noncoherent MIMO Radar for Location and Velocity Estimation: More Antennas Means Better Performance," *IEEE Trans. Signal Process.*, vol. 58, pp. 3661–3680, July 2010.
- [10] S. M. Kay, *Fundamentals of Statistical Signal Processing: Estimation Theory*. Prentice Hall, 1993.